*The American Journal of Pathology, Vol. 175, No. 4, October 2009*

*DOI: 10.2353/ajpath.2009.090108*

*Biomarkers, Genomics, Proteomics, and Gene Regulation*

# Lipopolysaccharide-Induced Epithelial Monoamine Oxidase Mediates Alveolar Bone Loss in a Rat Chronic Wound Model

Daisuke Ekuni,* James D. Firth,† Tarun Nayer,‡ Takaaki Tomofuji,* Toshihiro Sanbe,* Koichiro Irie,* Tatsuo Yamamoto,*§ Takashi Oka,¶ Zhenzi Liu,† Juergen Vielkind,‖** and Edward E. Putnins†

*From the Departments of Preventive Dentistry,* and Pathology and Pathobiology,¶ Okayama University Graduate School of Medicine, Dentistry and Pharmaceutical Sciences, Okayama, Japan; the Department of Oral Biological and Medical Sciences,† Faculty of Dentistry, the Department of Cancer Endocrinology,‖ British Columbia Cancer Research Centre, and the Department of Pathology and Laboratory Medicine,** University of British Columbia, Vancouver, Canada; the Michael Smith Genome Sciences Centre,‡ British Columbia Cancer Research Centre, Vancouver, Canada and the Department of Dental Sociology,§ Kanagawa Dental College, Yokosuka, Japan*

**Reactive oxygen species (ROS) production is an antimicrobial response to pathogenic challenge that may, in the case of persistent infection, have deleterious effects on the tissue of origin. A rat periodontal disease model was used to study ROS-induced chronic epithelial inflammation and bone loss. Lipopolysaccharide (LPS) was applied for 8 weeks into the gingival sulcus, and histological analysis confirmed the onset of chronic disease. Junctional epithelium was collected from healthy and diseased animals using laser-capture microdissection, and expression microarray analysis was performed. Of 19,730 genes changed in disease, 42 were up-regulated ≥4-fold. Three of the top 10 LPS-induced genes, monoamine oxidase B (MAO/B) and flavin-containing monooxygenase 1 and 2, are implicated in ROS signaling. LPS-associated induction of the ROS mediator $H_2O_2$, as well as MAO/B and tumor necrosis factor (TNF)-α levels were validated in the rat histological sections and a porcine junctional epithelial cell culture model. Topical MAO inhibitors significantly counteracted LPS-associated elevation of $H_2O_2$ production and TNF-α expression *in vivo* and *in vitro*, inhibited disease-associated apical migration and proliferation of junctional epithelium and inhibited induced systemic $H_2O_2$ levels and alveolar bone loss *in vivo*. These results suggest that LPS induces chronic wounds via elevated MAO/B-mediated increases in $H_2O_2$ and TNF-α activity by epithelial cells and is further associated with more distant effects on systemic oxidative stress and alveolar bone loss.** ***(Am J Pathol 2009, 175:1398–1409; DOI: 10.2353/ajpath.2009.090108)***

The production of microbicidal reactive oxygen species (ROS), a key feature of the innate immune system, has been best characterized in professional phagocytes.[1] Although epithelial cells are the first line of defense against bacterial challenge, the antimicrobial ROS properties of this cell type have been, to date, largely unstudied. Recently it has been shown that natural gut epithelial infection in *Drosophila* is associated with rapid ROS synthesis, but flies that lack normal ROS cycling capacity have increased mortality rates.[2] In the event of chronic infection, however, excessive ROS production may become toxic to the host. Gastric epithelial cells exposed to various strains of *Helicobacter pylori* showed a dose-dependent increase in ROS generation. Likewise ROS levels were greater in epithelial cells isolated from gastric mucosal biopsy specimens from *H. pylori*-infected subjects than in cells from uninfected individuals.[3] *H. pylori* strains bearing the *Cag* pathogenicity island are associated with greater peptic ulceration[4] and induce higher levels of ROS and activated apoptosis markers caspase 3 and 8 than isogenic *Cag* pathogenicity island-deficient mutants.[3] The pathogenicity island may act by elevating

Supported by Grants-in-Aid for Scientific Research (18791612 to D.E.) from the Ministry of Education, Culture, Sport, Science and Technology of Japan, a Genome Canada/Genome B.C. Cancer Genomics grant (to J.V.), and a Canadian Institutes of Health Research grant (MOP-82830 to E.P).

Accepted for publication July 7, 2009.

Address reprint requests to Edward E. Putnins, D.M.D., Ph.D., Oral Biological & Medical Sciences, Faculty of Dentistry, University of British Columbia, 2199 Wesbrook Mall, Vancouver, BC V6T 1Z3, Canada. E-mail: putnins@interchange.ubc.ca.

mitochondrial ROS formation[5], and, if so, monoamine oxidases (MAOs), which generate the ROS mediator $H_2O_2$ and are a component of the mitochondrial membrane found in most cell types in the body,[6] might be expected to be one of the sources.

Prolonged exposure to pathogenic bacteria and/or their secreted virulence factors may result in delayed wound closure and pathological tissue changes.[7] *In vitro*, lipopolysaccharide (LPS) derived from either *Pseudomonas aeruginosa* or *Escherichia coli* strongly inhibits epithelial migration and is therefore implicated as a factor in the failure of wound closure.[8] *In vivo*, periodontal disease offers a model of such chronic wound conditions. The periodontal sulcus is located in a space between the tooth and surrounding gingival tissue and is composed of junctional epithelium, which interfaces with periodontal soft and mineralized tissue. The recess of the sulcus favors population by an adherent bacterial biofilm and hence chronic challenge by virulence factors. Conversion of this biofilm to a Gram-negative, LPS-rich microbial population is associated with the conversion of the junctional to pocket epithelium, which is regarded as an early marker of disease initiation.[9] Periodontitis is associated with oxidative stress,[10] decreased total antioxidant status,[11] and/or increased lipid peroxidation in gingival crevicular fluid and saliva.[12]

Experimentally induced periodontitis provides a valuable model of chronic wounds and alveolar bone loss. Rats treated daily under anesthesia by application of *E. coli* LPS into the gingival sulcus showed disease as indicated by elongation of rete ridges and onset of apical migration of junctional epithelium at 8 weeks. Addition of *Streptomyces griseus* protease to the LPS treatment further potentiated the LPS-induced effects, yet protease treatment alone had no significant effect.[13] The LPS/protease model also established that the progressive development of disease was associated with apoptosis of adjacent fibroblasts and destruction of collagen fibers relative to both sham-treated and untreated (time 0) controls.[14] This model also demonstrated that elevated local and plasma oxidative stress, as measured by 8-hydroxydeoxyguanosine levels, was associated with chronic wound formation and alveolar bone loss.[15]

In this study, the established LPS/protease-induced rat chronic wound model[13–15] was used to analyze epithelial ROS signaling leading to alveolar bone loss relative to time 0 controls. First, epithelial tissues isolated by laser-capture microdissection were analyzed by expression microarray for transcriptional changes associated with the onset of epithelial disease and alveolar bone loss. Second, because microdissected disease epithelia were shown to have elevated infiltration of polymorphonuclear leukocyte (PMN) immune cells, consistent with the inflammatory process, pro-oxidative genes of interest, monoamine oxidase A (*Maoa*) and B (*Maob*) were validated both by RT-quantitative (q) PCR and at the protein level (MAO/A and MAO/B) in cell culture. This validation was done using a confirmed PMN-free primary culture of porcine junctional epithelia, both because isolation of sufficient rat junctional epithelia for culture was impractical and to confirm the conservation of the mechanism across species. Third, because tumor necrosis factor-$\alpha$ (TNF-$\alpha$) has been reported to be up-regulated in chronic wounds[16] and involved in bone loss,[17] LPS-associated ROS induction was assayed in association with elevated TNF-$\alpha$ protein expression both *in vivo* and *in vitro*. Fourth, the effects of LPS on TNF-$\alpha$ activity were further characterized *in vitro* using ROS inhibitors and MAO inhibitors. Finally, topically applied phenelzine, an MAO inhibitor, was tested *in vivo* for modulation of LPS-associated $H_2O_2$ production, TNF-$\alpha$ expression, PMN infiltration, systemic oxidative stress, and bone loss.

## Materials and Methods

### Animal Experiments

Animal experiments complied with guidelines of and were approved by the Animal Research Committee of The University of British Columbia and the Animal Research Control Committee of Okayama University Dental School. A rat periodontitis model was used as described previously: Animals were anesthetized daily using Isoflurane (Baxter, Toronto, ON, Canada), and then 25 $\mu$g/$\mu$l of serotype O55:B5 *E. coli* LPS (Sigma-Aldrich, St. Louis, MO) with 2.25 U/$\mu$l of *S. griseus* type XIV proteases (Sigma-Aldrich), which was used for acceleration of LPS penetration, resuspended in pyrogen-free water (ICN Biomedical Inc., Aurora, OH), was introduced by micropipette into the left and right palatal gingival sulcus of all three maxillary molars as described previously.[13,14] A total of 14 male Wistar strain rats (6 weeks old) were used per experiment, with seven animals in each of the time 0 control and 8-week treatment groups. In another experiment using 21 male Wistar strain rats, 4 weeks after LPS/protease treatment was begun in 14 animals, this group were randomly divided into two groups of seven animals each. Thereafter, in addition to LPS/protease treatment, one group of rats also received topical application of 0.5 $\mu$l of 250 mg/ml phenelzine (Sigma-Aldrich) in pyrogen-free water for 4 weeks. The third group of 7 rats received topical application of pyrogen-free water for 8 weeks.

### Tissue Preparation

Before death, rats were deeply anesthetized using Isoflurane and the right palatal gingival soft tissue was collected by sharp dissection, immediately embedded in optimal cutting temperature compound (Sakura Finetek USA, Inc., Torrance, CA), frozen in liquid nitrogen, and stored at −86°C until required. Sections from these blocks were subsequently used for laser dissection and processed for microarray analysis. After removal of the right palatal biopsy sample, rats were euthanized by intracardiac perfusion with 4% paraformaldehyde in 0.1 mol/L phosphate buffer (pH 7.4) under deep general anesthesia. After initial fixation, the left maxillary molar regions were resected *en bloc* from each rat. Tissues were decalcified with 10% tetrasodium-EDTA aqueous solution (pH 7.4) for 2 weeks at 4°C. Paraffin-embedded buccolingual 5-$\mu$m sections were made and used for morphometric and immunohistochemical analysis.

**Table 1.** Primer Sequences

| Gene | Accession | Sequence |
|---|---|---|
| *Maoa* | NM_001001640 | F: 5′-AGGAACGGAAGTTTGTAGGCGGAT-3′<br>R: 5′-ATAGGTGACAGGACACCTCAGCTT-3′ |
| *Maob* | AY596820 | F: 5′-TTACAAAGAGCCCTTCTGGAGGCA-3′<br>R: 5′-TGGAATCATCCAACGTGTAGGCGA-3′ |
| *Tnfa* | EU682384 | F: 5′-GCCCACGTTGTAGCCAATGTCAAA-3′<br>R: 5′-GTTGTCTTTCAGCTTCACGCCGTT-3′ |
| *Gapdh* | AF017079 | F: 5′-GCAAAGTGGACATTGTCGCCATCA-3′<br>R: 5′-CCGTGGAATTTGCCATGGGTAGAA-3′ |
| *Actb* | DQ452569 | F: 5′-AGCTGGAGTCTTTCTCGTGTTTGC-3′<br>R: 5′-TCACACGAGCCAGTGTTAGTACCT-3′ |

F, forward; R, reverse.

## *Morphometric Analysis*

Paraffin sections of 5-$\mu$m thickness were stained with H&E, and the distances from the cemento-enamel junction to the coronal aspect of the connective tissue attachment (epithelial migration) and from the cemento-enamel junction to the coronal margin of alveolar bone (bone loss) were measured using a microgrid at $\times$200 magnification. The number of PMNs was determined per 0.05 $mm^2$ under a magnification of $\times$400.[13] Means of histological data were calculated for each rat.

## *Gene Expression Analysis*

Serial 8-$\mu$m-thick cryosections were cut on the day of use using a cryostat (Cambridge Instruments, Heidelberg, Germany) onto membrane slides (Zeiss P.A.L.M., Bernried, Germany) from three blocks each of the control and experimental groups. Immediately before use slides were briefly thawed, stained with Mayer's hematoxylin (Sigma-Aldrich), rinsed with RNase-free $H_2O$, and drained. Slides were sequentially dehydrated through 75, 95, and 100% ethanol for 30 seconds each, transferred into xylene for 5 minutes, and air-dried for 5 minutes. Slides were immediately used for laser-capture dissection (Zeiss P.A.L.M.). Sufficient sections were collected to yield a minimum of $2 \times 10^6$ $\mu m^2$ of epithelia from each animal. Sections from each animal were pooled, and RNA was extracted using the RNeasy Micro Kit (Qiagen, Mississauga, ON, Canada). Amplified cRNA was produced and analyzed at Genome British Columbia (Vancouver, BC, Canada). Purified RNA was amplified using a GeneChip Expression 3′-Amplification Two-Cycle cDNA Synthesis Kit (Affymetrix, Santa Clara, CA), cRNA quality/quantity was assayed using a lab-on-a-chip/Bioanalyzer 2100 system (Agilent Technologies, Santa Clara, CA), and cRNA was subject to expression analysis using a GeneChip Rat Genome 230 2.0 Array (Affymetrix). Microarray data were analyzed using principal component and dChip software.[18] For RT-qPCR cell cultures were processed using an RNeasy Micro Kit as above. Template was synthesized using a SuperScript III First-Strand Synthesis Kit (Invitrogen, Carlsbad, CA). Primers of interest (Table 1) were designed from porcine sequences using software from and synthesized by Integrated DNA Technologies (Coralville, IA). qPCR was performed using Platinum SYBR Green qPCR Super Mix-UDG (Invitrogen), and primers were subjected to 50°C for 10 minutes with initial denaturation at 94°C for 10 minutes, followed by 35 cycles of denaturation for 10 seconds, annealing at 60°C for 15 seconds, and extension at 72°C for 20 seconds. Raw data were analyzed with a relative quantification software tool (REST) using two internal reference genes (*Gapdh* and *Actb*), and results are presented as fold change relative to controls.[19]

## *Immunohistochemistry*

Representative cryosections or deparaffinized sections were stained with the primary antibodies recognizing MAO/A, MAO/B (Santa Cruz Biotechnology, Inc., Santa Cruz, CA), and TNF-$\alpha$ (R&D Systems, Minneapolis, MN) in PBS/bovine serum albumin and Histofine Simple Stain MAX PO Kits (Nichirei Co., Tokyo, Japan). In brief, deparaffinized tissue sections or cryosections were immersed in methanol containing 0.3% $H_2O_2$ for 30 minutes to block endogenous peroxidase activity. The sections were treated with secondary antibody (Fab′)-conjugated peroxidase complex for 30 minutes. Peroxidase staining was performed for 5 to 10 minutes using a solution of 3,3′-diaminobenzidine tetrahydrochloride in 50 mmol/L Tris-HCl (pH 7.5) containing 0.001% $H_2O_2$. The sections were counterstained with Mayer's hematoxylin. Digital quantification was performed to segment the area of interest and determine the ratio of positive expression in a given area using the Scion Image (Scion Corp., Frederick, MD) computer program as described previously.[20]

## *Cell Culture Experiments*

Porcine ligament epithelial cells were isolated as described previously[21] and maintained in $\alpha$-minimal essential medium (Gibco BRL, Rockville, MD) supplemented with 15% fetal bovine serum (PAA Laboratories Inc., Etobicoke, ON, Canada). Cells were plated into 96-well plates for RT-qPCR or $H_2O_2$ assay, 24-well plates for immunostaining or TNF-$\alpha$ assay, or 35-mm dishes for flow cytometry. When cultures were 75% confluent, the cells were quiesced overnight in serum-free $\alpha$-minimal essential medium. Cells were treated with *E. coli* LPS (O55:B) at 12.5 to 1600 ng/ml. Long-term experiments of up to 2 weeks were performed with 2.5% serum and 250 ng/ml

LPS. In some experiments, cells were pretreated with *N*-acetylcysteine (10 to 80 mmol/L, 1 hour) or catalase (125 to 1000 U/ml, 1 hour) (Sigma-Aldrich) and thereafter with or without 800 ng/ml LPS. In other experiments, cells were treated with the MAO/B inhibitor *R*-(−)-deprenyl hydrochloride or the MAO/A+B inhibitor phenelzine sulfate salt (Sigma-Aldrich) at 3 to 100 $\mu$mol/L in the absence or presence of 800 ng/ml LPS.

### *TNF-$\alpha$ Quantitation*

Quantification of TNF-$\alpha$ levels in cell supernatant was performed using DuoSet enzyme-linked immunosorbent assay kits (R&D Systems). The 96-well microtiter plates were precoated with a monoclonal mouse anti-porcine TNF-$\alpha$ antibody. Then 200 ml of the samples was transferred to 96-well plates from 24-well plates, standards were applied and run in parallel, and all plates were incubated for 2 hours at room temperature. Plates were washed and further incubated with a biotinylated goat anti-porcine TNF-$\alpha$ antibody. The specifically bound antibody was detected by application of streptavidin-horseradish peroxidase. Peroxidase activity was visualized by the addition of tetramethylbenzidine substrate solution in $H_2O_2$. After 20 minutes of incubation, 2 N $H_2SO_4$ stop solution was added, and the plates were read at 450 nm.

### *Immunostaining and Flow Cytometry*

Semiconfluent, quiescent porcine ligament epithelial cultures were treated with increasing concentrations of LPS as above. Cells were recovered by trypsinization, neutralized with 10% serum, washed with PBS for flow cytometry or left *in situ* for immunostaining, and then fixed in 2% formaldehyde/5% sucrose for 1 hour at room temperature. Fixative was washed out three times with PBS, and then cells were blocked for 1 hour in hybridization buffer (3% bovine serum albumin, 0.2 mol/L glycine, and 0.1% saponin), which was also used in subsequent steps. Samples were incubated with MAO/A, MAO/B, or TNF-$\alpha$ antibody for 1 hour and then washed three times. Samples were incubated with Alexa Fluor 488-conjugated secondary antibody (Molecular Probes, Eugene, OR) and finally were washed three times in PBS. Five groups of 10,000 cells from triplicate experiments were analyzed using a FACSCalibur system (BD Biosciences, San Jose, CA) or by epifluorescence and were digitally recorded. Samples stained with secondary antibody alone were included to standardize results relative to autofluorescence.

### *ROS Quantitation*

Serum $H_2O_2$ levels were measured colorimetrically using the Amplex Red Kit (Molecular Probes). Fluorescence intensity was recorded with excitation in the range of 530 to 560 nm and emission of 590 nm. To directly detect ROS in cryosections or cultured cells, samples were incubated with 0.5 mg/ml 3,3-diaminobenzidine and 0.1 mol/L Tris-HCl, pH 7.6, alone ($H_2O_2$) or including 0.1 mg/ml $MnCl_2$ ($O_2^-$)[22] for 10 minutes and then were washed three times with PBS, counterstained with hematoxylin, washed three times with PBS again, fixed (2% paraformaldehyde, 5% sucrose, and PBS), and mounted. Images were digitally recorded under tungsten illumination and quantified as above. ROS scavenging was also tested cell-free with increasing concentrations of catalase, *R*-(−)-deprenyl hydrochloride or phenelzine sulfate incubated with $H_2O_2$ (1 mmol/L, room temperature, 1 hour) and then incubated with 3,3′-diaminobenzidine tetrahydrochloride as above and measured spectrophotometrically at 560 nm.

### *Statistical Analysis*

Data analysis was performed using a statistical software package (SPSS 15.0J for Windows, SPSS Japan, Tokyo, Japan). Data are expressed as means ± SD. Statistical analysis was performed using a Mann-Whitney *U*-test for comparison between the two groups ($P < 0.05$). Differences among the three groups were analyzed using a Kruskal-Wallis test followed by a Mann-Whitney *U*-test, using the Bonferroni correction to adjust probability ($P < 0.05/3 = 0.017$).

## *Results*

The previously established experimental periodontitis model was used with time 0 controls (healthy) and rats that received 8 weeks of daily applications of LPS/protease combined treatment to the gingival sulcus (disease).[13,14] The treated group exhibited apical migration of junctional epithelium characteristic of disease (Figure 1, A and D). As confirmed by morphology, cryosections from healthy (Figure 1, B and C) and diseased (Figure 1, E and F) rats were processed by laser-capture microscopy for the isolation of epithelium. Laser captures sections of about 2 million $\mu m^2$ of epithelium from each group were pooled, RNA was purified, and then sections were subjected to two rounds of amplification and cRNA synthesis (Figure 2). Far fewer sections were required from the disease group to reach the required total area because of increased epithelial proliferation associated with LPS treatment as shown in Figure 1. This response to bacterial challenge may be similar to the increased proliferation reported in gastric mucosal epithelia in response to *H. pylori* infections.[23] Total amplified cRNA and cRNA per unit area were highly consistent between healthy (control group) and diseased (8-week treatment group) animals (Figure 2A), and RNA yields from healthy (Figure 2B) and diseased (Figure 2C) rats showed consistent size profiles that ranged from 52 to 3891 nucleotides with a median size of 510 nucleotides for all samples, indicating that LPS treatment was not associated with increased RNA degradation.

Gene expression changes were assayed by subjecting cRNA from healthy and diseased animals to microarray analysis. Normalized data were first analyzed by principal component analysis, which showed that healthy and diseased samples grouped quite separately, but

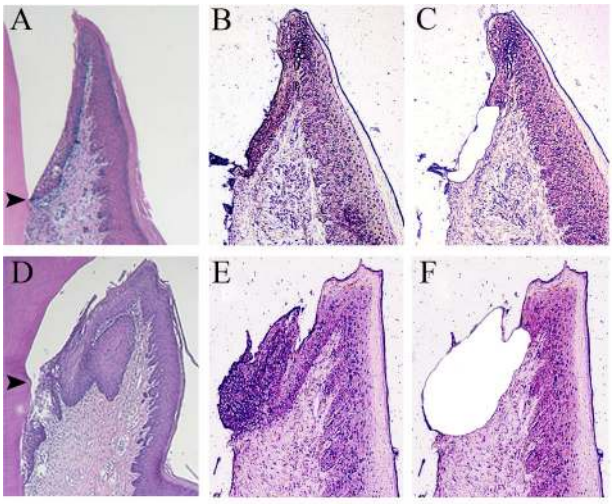


**Figure 1.** Microdissection of epithelia from healthy and LPS-induced chronically diseased tissues. LPS was applied daily to the palatal gingival sulcus of maxillary molars of male Wistar rats. Animals in each group ($n$ = 7) were sacrificed at time 0 (**A–C**) or 8 weeks (**D–F**). The maxilla were removed, decalcified, paraffin-embedded, sectioned, and stained with H&E. Representative samples are shown with the **black arrowheads** indicating the epithelial cell apical boundary, the cemento-enamel junction that is normally associated with health (**A**) or disease (**D**). From the same animals before sacrifice, palatal biopsy samples were removed under general anesthesia, embedded in optimal cutting temperature compound, frozen, cryosectioned, stained with hematoxylin, and processed for laser-capture microdissection of healthy (**B** and **C**) and disease-associated epithelial tissues (**E** and **F**). Scale bar = 200 $\mu$m.

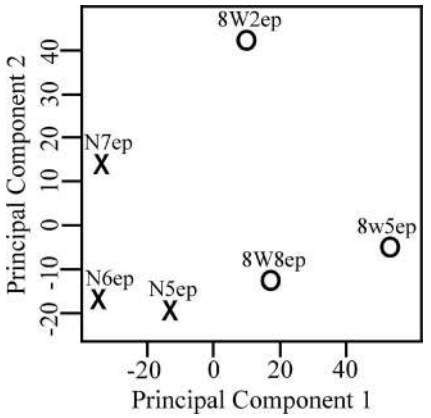


**Figure 3.** Principal component analysis of amplified cRNA. cRNA of 0-week control (N5–7ep) and 8-week LPS-treated groups (8W2ep, 8W5ep, and 8W8ep) was used for gene array analysis, and then samples were subjected to preliminary evaluation by principal component analysis to reduce multidimensional sets to a lower dimension for analysis. Analysis distribution showed that healthy and disease-associated samples were distinctively grouped. All three control samples were closely grouped and were included for further analysis. For the LPS-treated groups, two samples segregated closely but one (8W2ep) was classified as an outlier and hence was excluded from further analysis.

closely, within treatment groups, although one disease sample, number 2 rat in the 8 weeks of treatment group (8W2ep), was deemed to be somewhat of an outlier and was excluded from further analysis (Figure 3). Of particular interest, on the basis of ranked change, it was found that of the genes induced in response to disease onset (9031 of 19,730) only a very small number (42) showed a greater than fourfold increase in expression (Table 2). However, within the top 10 of this group, three genes, monoamine oxidase B (*Maob*, 5.72-fold) and flavin-containing monooxygenase 1 (*Fmo1,* 6.70-fold) and 2 (*Fmo2*, 7.26-fold) are involved in reactive oxygen signaling (Table 2). Further querying of the database for pro-oxidative genes in related pathways[24,25] revealed a generally consistent prevalence of increased expression (Table 2). Conversely, no antioxidant genes of interest[25] were found to be up-regulated but instead showed consistently decreased expression (Table 2). Taken together, these results indicate that LPS induced overall epithelial oxidative stress.

Because three top-ranked up-regulated genes had been implicated in the generation of ROS signaling intermediates,[24,25] we examined $H_2O_2$ (MAO activity) and superoxide (flavin-containing monooxygenase activity) levels *in vivo* and *in vitro*. The assay for $H_2O_2$ (3,3′-diaminobenzidine) and superoxide (3,3′-diaminobenzidine/manganese) showed that both were strongly induced in LPS-treated tissues (Figure 4A). Porcine epithelial cell (PLE) cultures have previously been established as a model for junctional epithelium.[26] Here, PLE cultures treated with LPS also showed strongly increased $H_2O_2$

A

Control (0 weeks)

| Block | N° of Sections | Total Area (μm²) | Total cRNA(μg) | cRNA/area(pg/μm²) | cRNA(μg/ul) |
|---|---|---|---|---|---|
| N5ep | 62 | 2,046,163 | 125.22 | 61.19 | 7.04 |
| N6ep | 62 | 2,023,570 | 133.82 | 66.12 | 7.74 |
| N7ep | 62 | 2,108,896 | 141.04 | 66.88 | 8.87 |

Lipopolysaccharide/Protease treated (8 weeks)

| Block | N° of Sections | Total Area (μm²) | Total cRNA(μg) | cRNA/area(pg/μm²) | cRNA(μg/ul) |
|---|---|---|---|---|---|
| 8W2ep | 24 | 1,964,254 | 131.62 | 67.00 | 7.39 |
| 8W5ep | 24 | 2,029,612 | 126.18 | 62.17 | 7.21 |
| 8W8ep | 24 | 2,308,086 | 183.24 | 79.39 | 9.91 |

B C

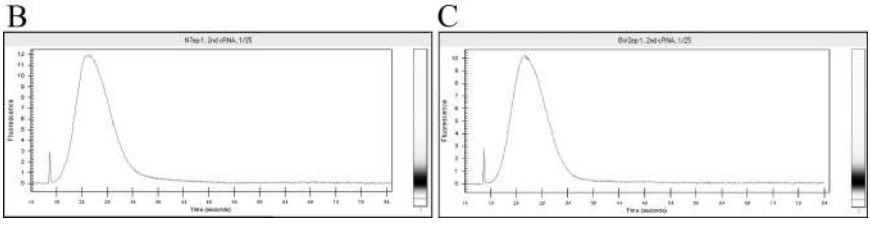

**Figure 2.** cRNA amplification of laser-capture microdissected healthy and disease-associated epithelia. Palatal biopsy samples from control and 8-week LPS-treated animals ($n$ = 3/group) were removed under general anesthesia, embedded in optimal cutting temperature compound, and frozen. Serial 8-$\mu$m cryosections were cut onto membrane slides, dehydrated, and processed for laser-capture microdissection. Sections from each animal were pooled, and total RNA was amplified through two cycles. Final cRNA was quantified and expressed per unit area of epithelia (**A**). Amplified cRNA from control (**B**) and 8-week treated (**C**) animals was compared for cRNA relative quality, cRNA size range (52 to 3891 nucleotides), and median size (510 nucleotides) for all groups.

**Table 2.** Gene Array Analysis of LPS-Induced Changes in Epithelial Gene Expression

| Genes changed | Fold change increased transcription | | | | Fold change decreased transcription | | | |
|---|---|---|---|---|---|---|---|---|
| | Total | 2–2.99× | 3–3.99× | >4× | Total | 2–2.99× | 3–3.99× | >4× |
| 19,730 | 9031 | 265 | 39 | 42 | 10,699 | 359 | 81 | 47 |

| Top 10 genes increased | Healthy mean | Healthy SE | Disease mean | Disease SE | Fold increase |
|---|---|---|---|---|---|
| Monoamine oxidase B | 192.11 | 16.71 | 1098.08 | 330.17 | 5.72 |
| LRP16 protein | 16.15 | 6.86 | 95.38 | 31.79 | 5.91 |
| Paraoxonase 3 | 111.00 | 36.70 | 693.64 | 257.86 | 6.25 |
| Epidermal growth factor-like protein 6 | 32.10 | 10.65 | 201.63 | 84.16 | 6.28 |
| Flavin-containing monooxygenase 1 | 95.65 | 29.21 | 641.29 | 170.15 | 6.70 |
| 4-Aminobutyrate aminotransferase | 46.14 | 26.68 | 323.57 | 72.50 | 7.01 |
| Flavin-containing monooxygenase 2 | 74.42 | 50.28 | 540.10 | 224.85 | 7.26 |
| Palate/lung/nasal carcinoma protein precursor | 148.96 | 59.85 | 1232.08 | 818.08 | 8.27 |
| Transcription factor AP-2$\beta$ (predicted) | 30.24 | 8.77 | 394.16 | 108.83 | 13.03 |
| Dihydropyrimidinase-like 3 | 9.11 | 0.92 | 233.95 | 68.29 | 25.69 |

| Pro-oxidative functions | Gene description | Symbol | RGD ID | Fold increase |
|---|---|---|---|---|
| NADPH-dependent oxidases | Flavin-containing mono-oxygenase 1 | *Fmo1* | 2622 | 6.70 |
| | Flavin-containing mono-oxygenase 2 | *Fmo2* | 628600 | 7.26 |
| | Flavin-containing mono-oxygenase 3 | *Fmo3* | 619761 | 3.93 |
| | Flavin-containing mono-oxygenase 4 | *Fmo4* | 628601 | 1.98 |
| Xenobiotic metabolism | Cytochrome P450 2/b/2 | *Cyp2b2* | 2467 | 1.50 |
| NADPH oxidases | NADP oxidase 1 | *Nox1* | 620598 | −1.37 |
| Amine oxidases | Monoamine oxidase A | *Maoa* | 61898 | 1.54 |
| | Monoamine oxidase B | *Maob* | 3041 | 5.72 |

| Anti-oxidative functions | Gene description | Symbol | RGD ID | Fold increase |
|---|---|---|---|---|
| $H_2O_2$ scavenger | Catalase | *Cat* | 2279 | −1.32 |
| | Metallothionein 3 | *Mt3* | 621252 | −2.31 |
| Superoxide dismutases | Superoxide dismutase 1 | *Sod1* | 3731 | −1.21 |
| | Superoxide dismutase 2 | *Sod2* | 3732 | −1.11 |
| NADP reduction | Glutathione reductase | *Gsr* | 621747 | −1.91 |
| Thioltransferase | Glutaredoxin 1 | *Glrx1* | 70951 | −1.21 |
| Heme reduction | Heme oxygenase (decycling) 1 | *Hmox1* | 2806 | −1.68 |
| | Biliverdin reductase A | *Blvra* | 620721 | −1.97 |

Oral junctional epithelia from control (0 weeks) and LPS-treated (8 weeks) rats was isolated by laser capture microscopy and pooled, and RNA was extracted. Amplified cRNA was subject to microarray expression assay using GeneChip Rat Genome 230 2.0 Array and dChip analysis software. Data are presented as a summary of changes in LPS-induce disease group: Total changes, top 10 genes by fold increase in expression, relevant pro-oxidative genes altered, and relevant anti-oxidant genes altered are shown.

RGD ID, Rat Genome Database identification number.

and superoxide positive staining (Figure 4B). In both cases the distribution of staining seemed consistent with previous reports of $H_2O_2$ extracellular diffusibility.[27] Digital quantitation of tissue and cell culture experiments showed that $H_2O_2$ and superoxide expression was significantly increased in both LPS-treated models ($P < 0.05$) (Figure 4C). PMNs are a major source of ROS, and LPS-induced PMN infiltration into the epithelial compartment is a characteristic of inflammation.[28] We assayed LPS-induced increases in PMNs in the epithelial compartment and a significant increase in PMNs was found in the 8-week treatment group ($P < 0.05$) (Figure 4D), consistent with the onset of inflammatory disease. To ascertain whether LPS-induced ROS could also be of epithelial origin, PLE cultures were first assayed for purity of the population. In addition to morphological confirmation, cell suspensions were immunostained with either the epithelium-specific marker cytokeratin 13 (CK13) or the PMN-specific marker integrin-$\beta_2$ (CD11) and assayed by flow cytometry. Exclusive staining of PLEs by cytokeratin 13 but not by CD11 (Figure 4E) confirmed the purity of the epithelial cell line. These data support an epithelial source of LPS-associated levels of ROS evident in Figure 4B.

We next addressed a possible molecular source for LPS-induced epithelial ROS. *Fmo2* in both humans[29] and rats[30] is known to be truncated and therefore nonfunctional; thus, it was not studied further. *Fmo1* is generally thought to be uninducible by xenobiotics, although recently it was reported to be up-regulated via the aryl hydrocarbon receptor.[31] *Maob* has previously been found to be inducible by 17$\beta$-estradiol in hamster kidney preceding carcinogenesis.[32] Flavin-containing monooxygenase 1 protein expression did not show any significant change at the protein level in either PLE culture or rat histological sections and so was not further studied (data not shown). However, in semiconfluent, quiescent control PLE cultures low constitutive MAO/B expression in a subpopulation of cells (horizontal gate) (Figure 5A) was detected by flow cytometry. Numbers of expressing cells and total MAO/B expression were clearly up-regulated in this subpopulation after 24 hours with 1000 ng/ml of LPS treatment (Figure 5B). The proportion of the total cell

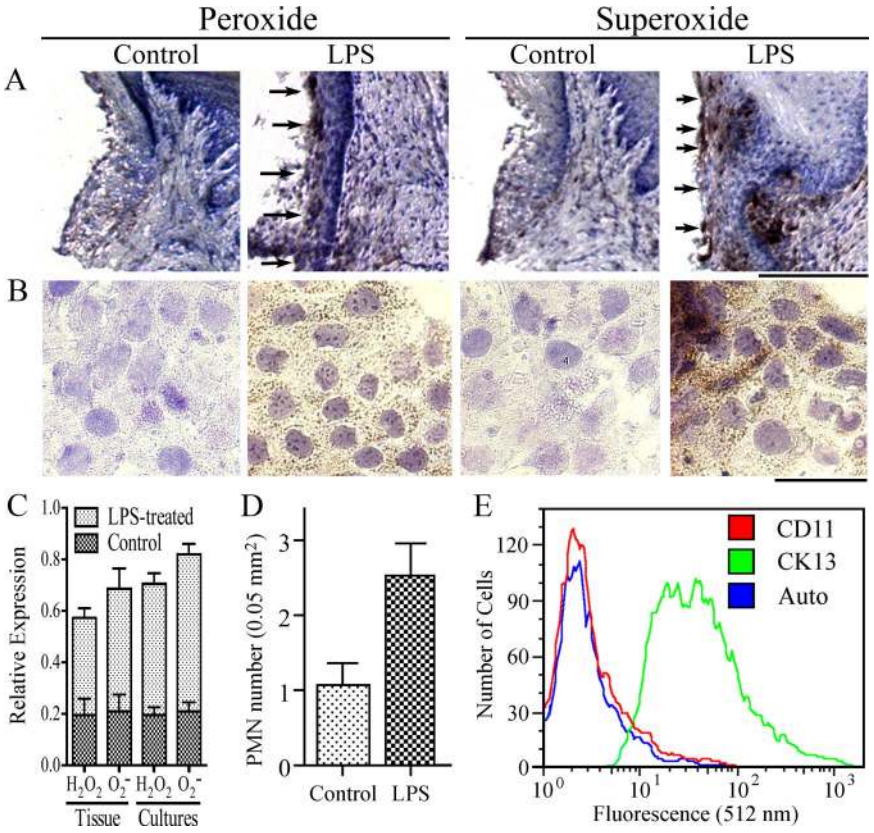


**Figure 4.** Detection of LPS-induced reactive oxygen species in healthy and diseased tissues. Reactive oxygen species were detected by incubation with 3,3-diaminobenzidine alone ($H_2O_2$) or in the presence of $MnCl_2$ (superoxide, $O_2^-$). **Arrows** indicate brown ROS staining. **A:** Cryosections of palatal biopsies from control and 8-week LPS-treated rats. Scale bar = 200 $\mu$m. **B:** Control and 24-hour LPS-treated primary cell cultures from porcine periodontal ligament epithelial cells. Scale bar = 50 $\mu$m. **C:** Digitized peroxide and superoxide relative expression levels were quantitated and are presented as mean ± SD. Cell culture data are representative of three independent experiments ($n = 6$) and for the animal experiment ($n = 7$) with differences between control and experimental groups significant at $P < 0.05$. **D:** Polymorphonuclear leukocyte infiltration into the epithelial compartment per 0.05 mm² was significantly increased ($P < 0.001$) in 8-week LPS-treated rats compared with time 0 controls; $n = 7$. **E:** Porcine epithelial cells were immunostained with either the polymorphonuclear leukocyte-specific marker integrin-$\beta_2$ (CD11) or the epithelial-specific marker cytokeratin 13 (CK13) and assayed by flow cytometry.

population responding to LPS by increasing MAO/B expression at 24 hours was found to be concentration-dependent and to plateau close to 1000 ng/ml with no discernible effect on MAO/A expression levels (Figure 5C). The effects of LPS on PLEs was studied for 2 weeks to simulate the *in vivo* chronic inflammatory challenge. PLEs were cultured in a combination of low serum (2.5%) and daily LPS treatment (250 $\mu$g/ml) that minimized both proliferation and apoptosis for up to 2 weeks (data not shown). Previously, ROS has been shown to play a central role of generating chronic inflammation and tissue damage in response to periodontal pathogens,[11] and chronic wounds are associated with significant up-regulation of TNF-$\alpha$.[16] In addition, targeted inhibition of MAOs has been shown to inhibit proinflammatory cytokine expression.[33,34] Therefore, this chronic *in vitro* model was

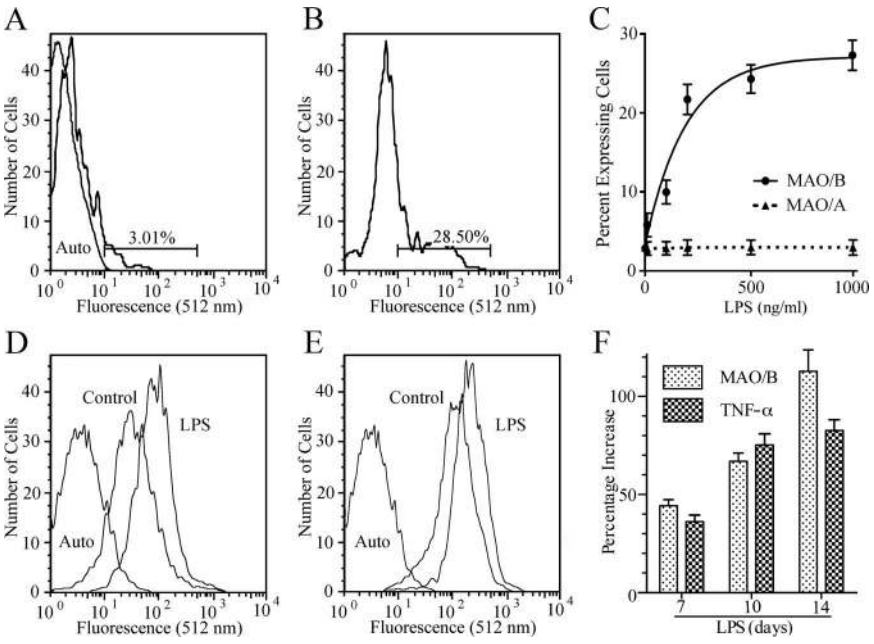


**Figure 5.** Validation of LPS-induced MAO/B and TNF-$\alpha$ protein up-regulation in LPS-treated cell cultures. Quiescent, semiconfluent primary cell cultures of porcine periodontal ligament epithelia were treated with various concentrations of LPS for 24 hours and compared with control cultures for changes in MAO/A or MAO/B expression by flow cytometry. The curve shift of the histogram of MAO/B was defined as percent expressing cell subpopulation (horizontal bars). **A:** Control. **B:** 1000 ng/ml LPS. **C:** Numbers of gated MAO/A or MAO/B high-expressing cells in response to increasing LPS concentration are presented as mean ± SD; $n = 6$. **D** and **E:** Epithelial model of chronic inflammation was cultured for 2 weeks with daily application of LPS (250 ng/ml) and then assayed by flow cytometry for MAO/B (**D**) and TNF-$\alpha$ (**E**). **F:** Epithelial expression of MAO/B and TNF-$\alpha$ was significantly induced ($P < 0.05$) by 7 days as assayed by flow cytometry and presented as mean ± SD; $n = 6$.

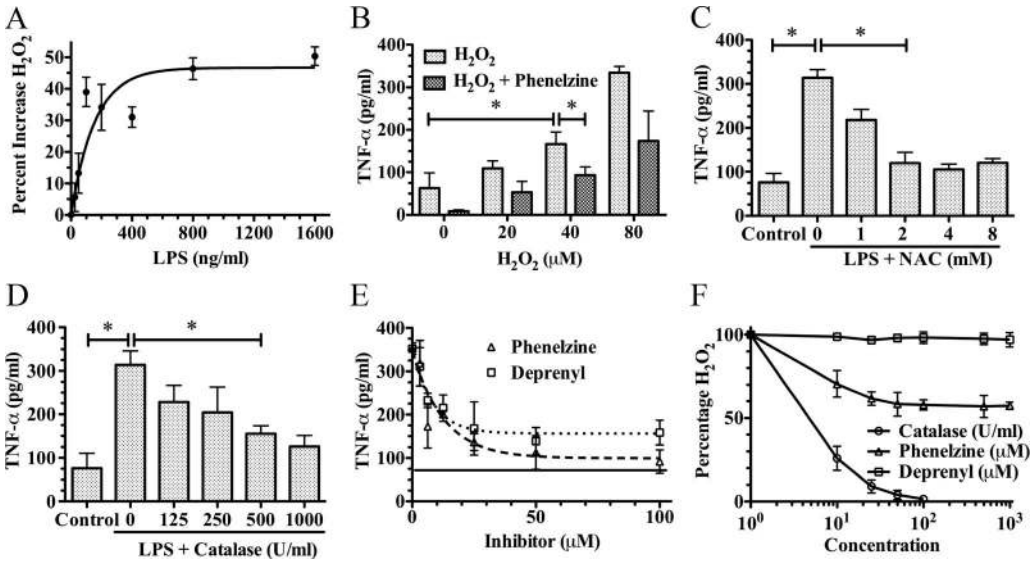


**Figure 6.** LPS regulation of TNF-α expression via $H_2O_2$ and MAO/B. Quiescent, semiconfluent primary cultures of porcine periodontal ligament epithelia were stimulated for 24 hours with increasing concentrations of LPS and assayed for $H_2O_2$ production (**A**), increasing concentrations of $H_2O_2$ alone or with phenelzine (25 μmol/L) (**B**), and assayed for up-regulation in TNF-α protein expression, 500 ng/ml LPS in the presence of increasing concentrations of catalase and then assayed for changes in TNF-α expression (**C**), and 500 ng/ml LPS in the presence of increasing concentrations of *N*-acetylcysteine (NAC) and then assayed for changes in TNF-α expression (**D**). **E:** Inhibition of LPS-induced TNF-α expression was assayed in the presence of the MAO/B inhibitor *R*-(−)-deprenyl hydrochloride or the MAO/A+B inhibitor phenelzine, and cultures were then assayed for changes in TNF-α expression. **F:** Scavenging of $H_2O_2$ in a cell-free system by increasing concentrations of catalase, *R*-(−)-deprenyl hydrochloride, or phenelzine was detected colorimetrically after incubation with 3,3-diaminobenzidine. Significant difference between groups bordering bars (*$P < 0.05$). Data are presented as mean ± SD; $n = 5$.

used to assay LPS-induced coincident changes in MAO/B and TNF-α protein expression. At 7, 10, and 14 days significant ($P < 0.05$) shifts of a large proportion of cell populations in flow cytometry assays were seen for both MAO/B (Figure 5, D and F) and TNF-α (Figure 5, E and F).

We next tested *in vitro* whether LPS regulation of TNF-α protein expression was mediated through MAO/B-mediated $H_2O_2$ generation. First, LPS was found to induce an increase in $H_2O_2$ production in a concentration-dependent manner (Figure 6A) and, further, exogenously added $H_2O_2$ induced a concentration-dependent increase in TNF-α protein expression but cotreatment with phenelzine significantly ($P < 0.05$) reduced induced levels (Figure 6B). Cotreatment of cultures with 500 ng/ml LPS and increasing concentrations of the ROS scavenger *N*-acetylcysteine (Figure 6C) or the $H_2O_2$ antagonist catalase (Figure 6D) largely ameliorated LPS induction of TNF-α present in cell culture media. Although exogenous catalase may not be highly cell permeable, $H_2O_2$ is, and scavenging it from the extracellular region should therefore be expected to reduce the intracellular oxidative load.[32] These data confirm the important role of ROS signaling in LPS induction of TNF-α expression in our culture model. We subsequently tested what impact MAO/B inhibition would have on 500 ng/ml LPS-induced TNF-α expression. Increasing concentrations of the MAO/B inhibitor deprenyl or MAO/A+B inhibitor phenelzine significantly ($P < 0.05$) reduced LPS-induced TNF-α expression (Figure 6E). As reported previously[35], we confirmed in a cell-free system that phenelzine but not deprenyl is also capable of partial direct $H_2O_2$ scavenging (Figure 6F). This finding could explain the increased ability of phenelzine over deprenyl in Figure 5E to reduce $H_2O_2$-elevated TNF-α

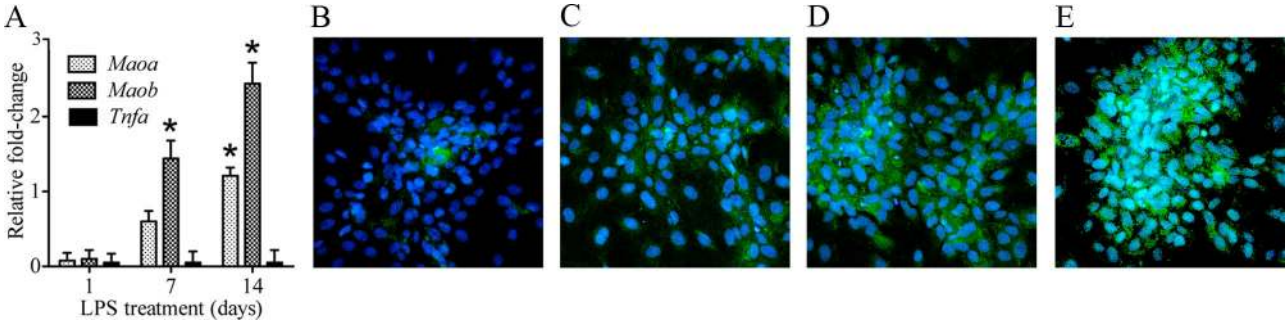


**Figure 7.** In vitro validation of LPS induction of MAO/B. Porcine epithelial cells were cultured for up to 2 weeks with or without daily treatment with LPS (250 ng/ml) and then were processed for RT-qPCR using primers designed from porcine mRNA sequences. Relative expression of target genes is presented as mean ± SD; $n = 6$ of fold change over untreated controls (**A**). Significant difference between groups (*$P < 0.05$). Parallel experiments were immunostained for relative MAO/B levels at 0 (**B**), 1 (**C**), 7 (**D**), and 14 (**E**) days.

levels. Phenelzine was chosen for further validation studies to avoid any potential compensation between the two isozymes during treatment.

To further investigate the mechanism linking LPS-induced MAO/B induction to increased TNF-$\alpha$ the long-term PLE model was used to assay changes to gene expression by RT-qPCR. At both 7 and 14 days LPS-treated cells showed significantly ($P < 0.05$) increased *Maob* expression and a more moderate increase of *Maoa*. However, no change in *Tnfa* was detectable (Figure 7A). With the same model the LPS-increased MAO/B expression was further confirmed by immunostaining of 0-, 1-, 7-, and 14-day experiments (Figure 7, B–E). Again no change was seen for TNF-$\alpha$ (data not shown). A post hoc survey of microarray data revealed that no LPS-induced change of TNF-$\alpha$ was detected (data not shown).

The role of MAO/B induction associated with TNF-$\alpha$ levels was further assayed in rat cryosections. LPS-treated 8-week samples showed MAO/B expression, which was most distinctly up-regulated in the epithelial compartment subpopulation (Figure 8A) similar to the onset of induction seen in the *in vitro* experiments. Consistent with its diffusibility,[27] $H_2O_2$ was detected over a wider area (Figure 8B), and TNF-$\alpha$ protein detection (Figure 8C) correlated spatially with $H_2O_2$. Chronic LPS topical application resulted in elevated levels for MAO/B, $H_2O_2$, and TNF-$\alpha$, and all three were significantly ($P < 0.017$) reduced in the phenelzine/LPS cotreated group (Figure 8, A–C, right panel, and D). Also *in vivo* we subsequently examined whether inhibition of MAO/B activity could counteract LPS-induced disease onset at both local and more distant foci. Paraffin-embedded sections from animals in control, LPS-treated, and LPS/phenelzine-treated groups were assayed for epithelial proliferation and alveolar bone loss using morphometric analysis as described previously.[13] In phenelzine cotreated animals, LPS-induced alveolar bone loss was significantly reduced coincident with a reduction of disease-associated junctional epithelial proliferation and migration ($P < 0.05$) (Figure 9, A and B). In addition, chronic LPS-associated local PMN infiltration and systemic $H_2O_2$ levels were also both significantly ($P < 0.05$) reduced with concomitant topical application of phenelzine (Figure 9C).

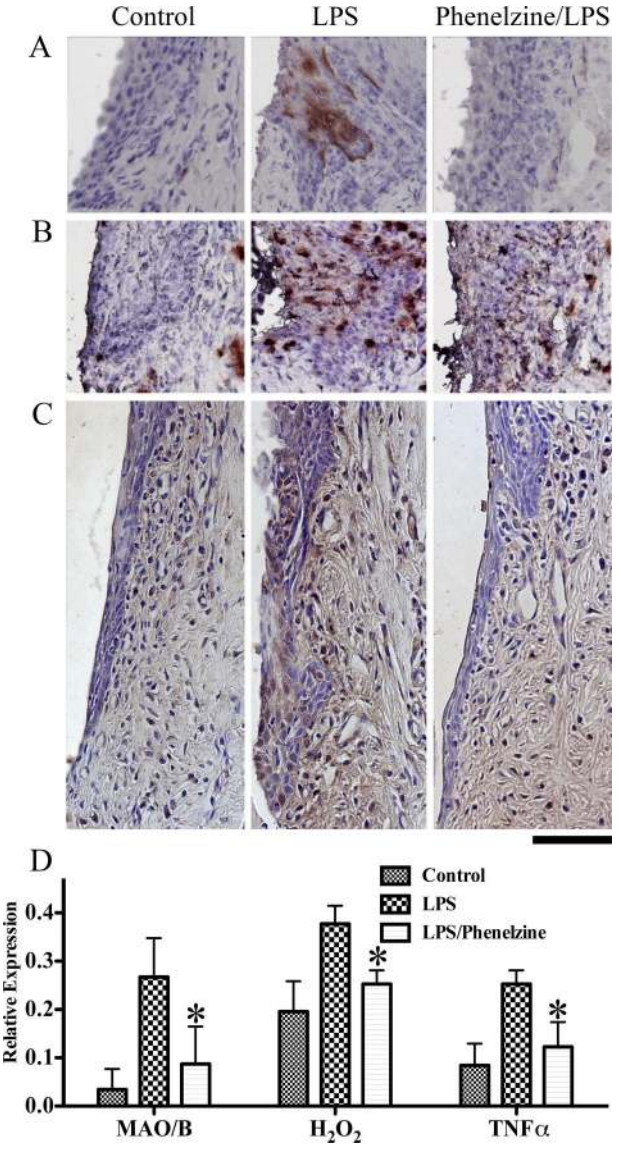


**Figure 8.** Inhibition of MAO/B, $H_2O_2$, and TNF-$\alpha$ expression by the MAO/A+B inhibitor phenelzine. Control, 8-week LPS-treated or LPS in the presence of topical phenelzine-treated rats were sacrificed, and palatal biopsies were processed by cryosectioning and immunohistochemical analysis followed by counterstaining. Brown color reveals staining for MAO/B (**A**), colorimetric staining for $H_2O_2$ (**B**), and staining for TNF-$\alpha$ (**C**). Scale bar = 100 $\mu$m. **D**: Digital quantification of histochemical staining of the epithelial compartment in control and treated groups. Data are presented as mean ± SD; $n = 7$. Relative expression of MAO/B, $H_2O_2$, and TNF-$\alpha$ in the phenelzine-treated group was significantly reduced compared with the LPS-treated group (*$P < 0.017$).

## *Discussion*

Numerous studies have assayed the effects of LPS by microarray analysis but, to date, only three have tested effects on normal epithelia. First, intramammary infusion of *E. coli* LPS for 4 hours in a mouse model identified 489 of 23,000 genes changed in whole mammary tissue. LPS binding protein CD14, chemokines CXCL1, CXCL2, and S100A8, and the acute-phase protein SAA3 were among the most significantly elevated (≥1.77), and these results were validated in mammary epithelial cell culture by Northern analysis.[36] Second, bovine mammary epithelial cell cultures stimulated with *E. coli* LPS for 6 hours identified 9 of 1278 transcripts induced (>1.25 times). Four of these, cytokines regulated upon activation, normal T cell expressed and secreted/CCL5, interleukin-6, and CXL5, and protease T-PA, were validated by Northern analysis.[37] Third, intraperitoneal injection of *E. coli* LPS in both rats and mice identified 10 genes from whole liver tissue that increased (>3 times) at 6 hours, of which the top-ranked, acute-phase protein lipocalin 24p3, was subsequently validated using LPS-treated type II alveolar epithelial cells.[38]

To study epithelial cell responses to a chronic inflammatory challenge we used a timed periodontal disease model,[13–15] which offered several experimental advan-

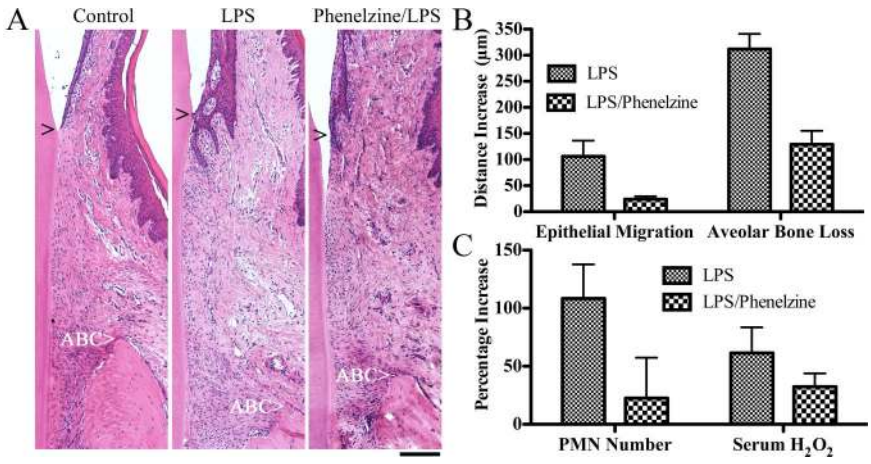


**Figure 9.** Topical phenelzine reduction of LPS-induced morphological indicators of disease, polymorphonuclear leukocyte infiltration and peripheral serum $H_2O_2$. **A:** Control rats or rats treated for 8 weeks with LPS alone or LPS in the presence of phenelzine were sacrificed and subjected to morphometric analysis ($n = 7$ per group). Epithelial migration was measured as the distance from the cemento-enamel junction (**arrowhead**) apically along the root surface. Bone loss was measured as an increase in the distance between the cemento-enamel junction to the crest of the existing alveolar bone (ABC). Scale bar = 100 $\mu$m. **B:** LPS-induced junctional epithelial migration and bone loss were both significantly reduced in phenelzine-treated animals ($P < 0.001$). **C:** LPS-induced polymorphonuclear leukocyte number per 0.05 mm$^2$ was significantly increased ($P < 0.001$) over that for untreated controls and significantly reduced from LPS-induced levels in the presence of phenelzine ($P < 0.001$). Serum $H_2O_2$ significantly induced by LPS ($P < 0.001$) as measured by phenylenediamine oxidation was significantly reduced ($P < 0.017$) in the presence of phenelzine.

tages. The direct application of *E. coli* LPS to the sulcus around a tooth enhanced epithelial suffusion and modeled normal disease pathobiology. Progression of chronic inflammation over 8 weeks could be confirmed by histological changes to junctional epithelium and eventual bone loss consistent with the diseased state. Precise laser-capture microscopy permitted microarray analysis specific to healthy and diseased epithelium. From this it was found that of the 42 genes most induced, three of the top 10, *Maob*, *Fmo1*, and *Fmo2*, are associated with generation of ROS signaling mediators.[24] Interestingly, *Maob* and *Fmo1* were also significantly up-regulated in gene chip analysis of atrial fibrillation-induced oxidative stress.[24] This is the first described induction of FMO enzymes within periodontal tissues and clarifies a previously described increase in MAO expression in periodontal tissues as most probably being MAO/B up-regulation.[39] Analysis was focused to validate up-regulation of MAO/B protein levels in histological sections of the same experimental animals and in porcine periodontal epithelial cell cultures previously established as a model for junctional epithelia.[26] LPS-induced epithelial MAO/B protein staining of tissue sections and epithelial cell cultures both identified a subpopulation of epithelial cells that were the most highly responsive.

MAO/A and MAO/B are found bound to the outer membrane of mitochondria in most cell types in the body and are the major enzymes catalyzing the oxidative deamination of monoamine neurotransmitters such as dopamine, adrenaline/noradrenaline, and serotonin.[6] In a previous study, C6 glioma cells treated with LPS were assayed for MAO/A and MAO/B activity, but no change was detected,[40] making the present study the first to date to detect such an effect. Oxidative deamination by MAO/B generates $H_2O_2$,[41] and consistent with this finding, $H_2O_2$ was elevated in diseased tissue sections and in our LPS-treated cell culture model. $H_2O_2$ along with other ROS participate in cell signaling and/or injury.[42] In addition, $H_2O_2$ is lipid-soluble and diffuses across biological membranes and has been shown to be a diffusible paracrine mediator for signal crosstalk between epithelial and stromal tissue.[27] Consistent with these findings we found LPS-induced $H_2O_2$ staining to be somewhat diffuse from sites of MAO/B staining. However, we also showed increased PMN infiltration into the epithelial compartment, consistent with chronic inflammation,[28] and this may be another $H_2O_2$ source.

The mechanism by which MAO up-regulation and subsequent therapeutic inhibition may contribute to this chronic inflammatory disease progression and inhibition, respectively, is significant. Previously it was postulated that remission of rheumatoid arthritis in patients taking MAO inhibitors may be due to inhibition of prostaglandin $E_2$ synthesis.[43] Subsequently, two cases were described in which the MAO inhibitor phenelzine induced remission in patients with another chronic inflammatory disease, Crohn's disease.[34] It was postulated that MAO inhibitors may inhibit these diseases by blocking TNF levels, but no evidence was presented.[44] However, further evidence begins to support this hypothesis. First, MAO/B levels are closely related to the pathogenesis of Parkinson's disease and up-regulation of TNF-$\alpha$ and interleukin-6 mRNA was increased in the hippocampus of Parkinson's patients.[45,46] MAO/B inhibitors are effective for the treatment of Parkinson's disease, both through their direct effect on MAO/B and in part by also activating multiple factors for anti-oxidative stress including anti-inflammatory cytokines.[45] Second, the MAO/A inhibitor moclobemide inhibited the unstimulated production of TNF-$\alpha$ and interleukin-8 in whole blood from healthy volunteers and enhanced the LPS-stimulated production of the anti-inflammatory cytokine interleukin-10.[33] However, the impact MAO/B inhibitors may have on LPS-induced cytokine expression in oral tissues has not been evaluated. In our *in vivo* chronic inflammatory disease model we found that LPS-induced TNF-$\alpha$ expression was largely abrogated by inhibition of MAO/B activity. Differences in our data compared with previous reports suggest that tissue-specific differences in LPS induction of MAO/A versus B expression and regulation may exist.

In our cell culture model $H_2O_2$ induced TNF-$\alpha$ protein expression in a concentration-dependant manner, and it was effectively inhibited by treatment with the $H_2O_2$ antagonist catalase and the ROS scavenger *N*-acetylcysteine. Similarly, LPS-induced TNF-$\alpha$ *in vivo* was significantly reduced by cotreatment with phenelzine. Previously it was shown that LPS induced ROS coordinates TNF-$\alpha$ production through I$\kappa$B kinase complex regulation of transcription factor nuclear factor-$\kappa$B.[47] Subsequently, LPS-induced TNF-$\alpha$ expression was largely inhibited by deprenyl (MAO/B inhibitor) but almost completed inhibited by phenelzine (MAO/A+B inhibitor). In a cell-free system we confirmed that phenelzine is also an $H_2O_2$ scavenger,[35] and that this characteristic may potentiate its antioxidant effect as an MAO inhibitor. However, neither microarray or RT-qPCR data revealed any significant LPS-induced changes in *Tnfa* transcription. Previously it was reported that increased TNF-$\alpha$ activity during inflammation may be due to post-translational activation of the prohormone rather than transcriptional up-regulation. Among candidates for LPS-induced TNF-$\alpha$ converting enzyme function in mouse myeloid cells *in vivo* is primarily ADAM 17, although ADAM 10 and 19, matrix metalloproteinase 7 and proteinase 3, are also TNF-$\alpha$ converting enzyme candidates.[48] Our microarray data showed some increase in ADAM 10 (1.82-fold) and ADAM 17 (1.16-fold). The accentuated detection of elevated TNF-$\alpha$ at the protein level may be due in part to the fact that the antibody is raised against an activated epitope. The elucidation of TNF-$\alpha$ activation in our model remains a subject for further enquiry.

These data provide additional support that MAO inhibitors do have a dramatic impact on proinflammatory cytokine expression, and their inhibition was best achieved using a drug that blocks both isoenzymes and scavenges ROS. *In vivo*, topical application of phenelzine significantly reduced classic outcomes of the periodontal epithelial disease process including proliferation and apical migration, PMN infiltration, an elevated serum oxidative load, and perhaps, most important, alveolar bone loss. TNF-$\alpha$, as one of the major cytokines driving inflammation, can directly promote osteoclastogenesis via binding to TNF receptor 1 on osteoclast precursor cells or indirectly via induction or macrophage colony-stimulating factor and receptor activator for nuclear factor $\kappa$B ligand on mesenchymal cells.[17] It further functions to direct homing, migration, and fusion of the precursor cells to mature bone-resorbing osteoclasts.[49] Moreover, TNF-$\alpha$ induction of Smurf-mediated degradation of Runx2 leads to the inhibition of osteoblast activity in restoring bone.[50] In this study, alveolar bone loss in LPS-treated rats was largely reduced by the MAO inhibitor phenelzine in association with strongly reduced ROS ($H_2O_2$) and TNF-$\alpha$ expression in the junctional epithelium.

In conclusion, this study provides the first evidence that in LPS-induced chronic epithelial wounds ROS generation, MAO/B expression, and TNF-$\alpha$ activity are upregulated. Furthermore, the progression of epithelial disease correlated with more distant alveolar bone loss. Both disease aspects were strongly reduced by the MAO inhibitor phenelzine via reduced MAO/B $H_2O_2$ generation and direct scavenging of $H_2O_2$. These data suggest that the mechanism by which MAO inhibitors alleviate the symptoms of several chronic inflammatory diseases (ie, Crohn's disease, rheumatoid arthritis, Parkinson's disease, and now experimental periodontal disease) may be largely a reduction in the levels of ROS molecules that can induce proinflammatory cytokine expression.

## Acknowledgment

We thank Ms. Pat Allard and Mr. John Fee for their technical assistance.

## References

1. Rosen H, Crowley JR, Heinecke JW: Human neutrophils use the myeloperoxidase-hydrogen peroxide-chloride system to chlorinate but not nitrate bacterial proteins during phagocytosis. J Biol Chem 2002, 277:30463–30468
2. Ha E-M, Oh C-T, Ryu J-H, Bae Y-S, Kang S-W, Jang I-H, Brey PT, Lee WJ: An antioxidant system required for host protection against gut infection in Drosophila. Dev Cell 2005, 8:125–132
3. Ding S-Z, Minohara Y, Fan XJ, Wang J, Reyes VE, Patel J, Dirden-Kramer B, Boldogh I, Ernst PB, Crowe SE: Helicobacter pylori infection induces oxidative stress and programmed cell death in human gastric epithelial cells. Infect Immun 2007, 75:4030–4039
4. Blaser MJ, Perez-Perez GI, Kleanthous H, Cover TL, Peek RM, Chyou PH, Stemmermann GN, Nomura A: Infection with Helicobacter pylori strains possessing cagA is associated with an increased risk of developing adenocarcinoma of the stomach. Cancer Res 1995, 55:2111–2115
5. Handa O, Naito Y, Yoshikawa T: CagA protein of Helicobacter pylori: a hijacker of gastric epithelial cell signaling. Biochem Pharmacol 2007, 73:1697–1702
6. Weyler W, Hsu YP, Breakefield XO: Biochemistry and genetics of monoamine oxidase. Pharmacol Ther 1990, 47:391–417
7. Robson MC, Kucukcelebi A, Carp SS, Hayward PG, Hui PS, Cowan WT, Ko F, Cooper DM: Maintenance of wound bacterial balance. Am J Surg 1999, 178:399–402
8. Loryman C, Mansbridge J: Inhibition of keratinocyte migration by lipopolysaccharide. Wound Rep Reg 2007, 16:45–51
9. Bosshardt DD, Lang NP: The junctional epithelium: from health to disease. J Dent Res 2005, 84:9–20
10. Akalın FA, Baltacıoğlu E, Alver A, Karabulut E: Lipid peroxidation levels and total oxidant status in serum, saliva and gingival crevicular fluid in patients with chronic periodontitis. J Clin Periodontol 2007, 34:558–565
11. Chapple IL, Brock GR, Milward MR, Ling N, Matthews JB: Compromised GCF total antioxidant capacity in periodontitis: cause or effect? J Clin Periodontol 2007, 34:103–110
12. Tomofuji T, Azuma T, Kusano H, Sanbe T, Ekuni D, Tamaki N, Yamamoto T, Watanabe T: Oxidative damage of periodontal tissue in the rat periodontitis model: effects of a high-cholesterol diet. FEBS Lett 2006, 580:3601–3604
13. Ekuni D, Yamamoto T, Yamanaka R, Tachibana K, Watanabe T: Proteases augment the effects of lipopolysaccharide in rat gingiva. J Periodont Res 2003, 38:591–596
14. Ekuni D, Tomofuji T, Yamanaka R, Tachibana K, Yamamoto T, Watanabe T: Initial apical migration of junctional epithelium in rats following application of lipopolysaccharide and proteases. J Periodontol 2005, 76:43–48
15. Ekuni D, Tomofuji T, Tamaki N, Sanbe T, Azuma T, Yamanaka R, Yamamoto T, Watanabe T: Mechanical stimulation of gingiva reduces plasma 8-OHdG level in rat periodontitis. Arch Oral Biol 2008, 53:324–329
16. Streit M, Beleznay Z, Braathen LR: Topical application of the tumour necrosis factor-$\alpha$ antibody infliximab improves healing of chronic wounds. Int Wound J 2006, 3:171–179
17. Lam J, Takeshita S, Barker JE, Kanagawa O, Ross FP, Teitelbaum SL:

TNF-α induces osteoclastogenesis by direct stimulation of macrophages exposed to permissive levels of RANK ligand. J Clin Invest 2000, 106:1481–1488
18. Li C: Automating dChip: toward reproducible sharing of microarray data analysis. BMC Bioinformatics 2008, 9:231
19. Pfaffl MW, Horgan GW, Dempfle L: Relative expression software tool (REST) for group-wise comparison and statistical analysis of relative expression results in real-time PCR. Nucleic Acids Res 2002, 30:e36
20. Ekuni D, Firth JD, Putnins EE: Regulation of epithelial cell growth factor receptor protein and gene expression using a rat periodontitis model. J Periodontal Res 2006, 4:340–349
21. Brunette DM, Melcher AH, Moe HK: Culture and origin of epithelium-like and fibroblast-like cells from porcine periodontal ligament explants and cell suspensions. Arch Oral Biol 1976, 21:393–400
22. Kerver ED, Vogels IM, Bosch KS, Vreeling-Sindelarova H, Van den Munckhof RJ, Frederiks WM: In situ detection of spontaneous superoxide anion and singlet oxygen production by mitochondria in rat liver and small intestine. Histochem J 1997, 29:229–237
23. Lynch DAF, Mapstone NP, Clarke AMT, Sobala GM, Jackson P, Morrison L, Dixon MF, Quirke P, Axon ATR: Cell proliferation in Helicobacter pylori associated gastritis and the effect of eradication therapy. Gut 1995, 36:346–350
24. Kim YH, Lim DS, Lee JH, Shim WJ, Ro YM, Park GH, Becker KG, Cho-Chung YS, Kim MK: Gene expression profiling of oxidative stress on atrial fibrillation in humans. Exp Mol Med 2003, 35:336–49
25. Wesseling S, Joles JA, van Goor H, Bluyssen HA, Kemmeren P, Holstege FC, Koomans HA, Braam B: Transcriptome-based identification of pro- and antioxidative gene expression in kidney cortex of nitric oxide-depleted rats. Physiol Genomics 2007, 28:158–167
26. Pan Y-M, Firth JD, Salonen JI, Uitto, V-J: Multilayer culture of periodontal ligament epithelial cells: a model for junctional epithelium. J Periodont Res 1995, 30: 97–107
27. Waghray M, Cui Z, Horowitz JC, Subramanian IM, Martinez FJ, Toews GB, Thannickal VJ: Hydrogen peroxide is a diffusible paracrine signal for the induction of epithelial cell death by activated myofibroblasts. FASEB J 2005, 19:854–856
28. Beatty WL, Sansonetti PJ: Role of lipopolysaccharide in signaling to subepithelial polymorphonuclear leukocytes. Infect Immun 1997, 65:4395–4404
29. Dolphin CT, Beckett DJ, Janmohamed A, Cullingford TE, Smith RL, Shephard EA, Phillips IR: The flavin-containing monooxygenase 2 gene (FMO2) of humans, but not of other primates encodes a truncated, nonfunctional protein. J Biol Chem 1998, 273:30599–30607
30. Lattard V, Longin-Sauvageon C, Krueger SK, Williams DE, Benoit E: The FMO2 gene of laboratory rats, as in most humans, encodes a truncated protein. Biochem Biophys Res Commun 2002, 292:558–563
31. Celius T, Roblin S, Harper PA, Matthews J, Boutros PC, Pohjanvirta R, Okey AB: Aryl hydrocarbon receptor-dependent induction of flavin-containing monooxygenase mRNAs in mouse liver. Drug Metab Dispos 2008, 36:2499–2505
32. Sarabia SF, Liehr JG: Induction of monoamine oxidase B by 17β-estradiol in the hamster kidney preceding carcinogenesis. Arch Biochem Biophys 1998, 355:249–253
33. Lin A, Song C, Kenis G, Bosmans E, De Jongh R, Scharpé S, Maes M: The in vitro immunosuppressive effects of moclobemide in healthy volunteers. J Affect Disord 2000, 58:69–74
34. Kast RE: Crohn's disease remission with phenelzine treatment. Gastroenterology 1998, 115:1034–1035
35. Lee CS, Han ES, Lee WB: Antioxidant effect of phenelzine on $MPP^+$-induced cell viability loss in differentiated PC12 cells. Neurochem Res 2003, 28:1833–1841
36. Zheng J, Watson AD, Kerr DE: Genome-wide expression analysis of lipopolysaccharide-induced mastitis in a mouse model. Infect Immun 2006, 74:1907–1915
37. Pareek R, Wellnitz O, Van Dorp R, Burton J, Kerr D: Immunorelevant gene expression in LPS-challenged bovine mammary epithelial cells. J Appl Genet 2005, 46:171–177
38. Sunil VR, Patel KJ, Nilsen-Hamilton M, Heck DE, Laskin JD, Laskin DL: Acute endotoxemia is associated with upregulation of lipocalin 24p3/Lcn2 in lung and liver. Exp Mol Pathol 2007, 83:177–87
39. Satyanarayana M, Rajeswari KR: Biogenic amines in human gingiva in healthy and inflamed states. Indian J Dent Res 1990, 2:170–173
40. Mazzio E, Becker A, Soliman KFA: Inflammation and inducible nitric oxide synthase have no effect on monoamine oxidase activity in glioma cells. Biochem Pharmacol 2003, 65:1719–1727
41. Werner P, Cohen G: Glutathione disulfide (GSSG) as a marker of oxidative injury to brain mitochondria. Ann NY Acad Sci 1993, 679:364–369
42. Thannickal VJ, Day RM, Klinz SG, Bastien MC, Larios JM, Fanburg BL: Ras-dependent and -independent regulation of reactive oxygen species by mitogenic growth factors and TGF-β1. FASEB J 2000, 14:1741–1748
43. Lieb J: Remission of rheumatoid arthritis and other disorders of immunity in patients taking monoamine oxidase inhibitors. Int J Immunopharmacol 1983, 5:353–357
44. Altschuler EL: Monoamine oxidase inhibitors in rheumatoid arthritis—anti-tumor necrosis factor? Int J Immunopharmacol 2000, 5:353–357
45. Nagatsu T, Sawada M: Molecular mechanism of the relation of monoamine oxidase B and its inhibitors to Parkinson's disease: possible implications of glial cells. J Neural Transm Suppl 2006, 71:53–65
46. Sawada M, Imamura K, Nagatsu T: Role of cytokines in inflammatory process in Parkinson's disease. J Neural Transm Suppl 2006, 70:373–381
47. Sanlioglu S, Williams CM, Samavati L, Butler NS, Wang G, McCray PB Jr, Ritchie TC, Hunninghake GW, Zandi E, Engelhardt JF: Lipopolysaccharide induces Rac1-dependent reactive oxygen species formation and coordinates tumor necrosis factor-α secretion through IKK regulation of NF-κB. J Biol Chem 2001, 276:30188–30198
48. Horiuchi K, Kimura T, Miyamoto T, Takashi H, Lkada Y, Toyama Y, Blobel CP: Cutting edge: TNF-α-converting enzyme (TACE/ADAM17) inactivation in mouse myeloid cells prevents lethality from endotoxin shock. J Immunol 2007, 179:2686–2689
49. Ritchlin CT, Haas-Smith SA, Li P, Hicks DG, Schwarz EM: Mechanisms of TNF-α- and RANKL-mediated osteoclastogenesis and bone resorption in psoriatic arthritis. J Clin Invest 2003, 111:821–831
50. Kaneki H, Guo R, Chen D, Yao Z, Schwarz EM, Zhang YE, Boyce BF, Xing L: Tumor necrosis factor promotes Runx2 degradation through up-regulation of Smurf1 and Smurf2 in osteoblasts. J Biol Chem 2006, 281:4326–4333